Optimisation of sintering processes for porcelain using in-situ measuring methods

C. Dannert, B. Durschang, F. Raether *; F.H. Becker **
* Fraunhofer-Institut Silicatforschung, Neunerplatz 2, 97082 Würzburg, Germany
** Riedhammer GmbH, Klingenhofstr. 72, 90411 Nürnberg, Germany

Abstract

By monitoring the thermal conductivity of ceramic materials during sintering, direct insight into the microstructural evolution can be gained. Using an in-situ thermooptical measuring system for measurement of thermal conductivities and densification rates and a high-temperature X-ray diffractometer, sintering mechanisms of porcelain have been examined. For the investigation of fast biscuit and glost firing cycles of whiteware, a firing process of a continuosly gas fired kiln with a firing atmosphere containing water vapour was simulated in a resistance heated laboratory furnace. The sintering properties deviate significantly from results obtained in dry air. From densification data, a „kinetic field" for the glost firing of whiteware has been set up to calculate optimal fast firing cycles and to determine the activation energy for the densification. The activation energy increases in the intermediate sintering stage.

Keywords: thermal conductivity, whiteware, fast firing, water vapour, atmosphere, kinetic field

1. Introduction

Industrial firing of porcelain is done in gas-heated kilns in a two-stage process. The green porcelain body is first biscuit fired up to 1000°C to improve its handling capabilities. After being glazed it is then glost fired up to 1400°C. To save energy and time, one or both of the firing cycles nowadays are carried out as „fast firing" cycles. Problems arise with respect to shape consistency (1) when both firing cycles are performed „fast". Although many authors have examined the effect of raw materials on the firing behaviour in fast firing of porcelain ((1), for overview see (2)), the effect of the firing atmosphere containing water vapour and reducing gas components on the microstructure has often been neglected. In this work, the evolution of the ceramic microstructure during sintering of porcelain and the influence of water vapour atmospheres onto it is investigated. For that in-situ measuring methods, e.g. measurements of thermal conductivity (3, 4, 5) and shrinkage (dilatometry) have been used.

Triaxial porcelain is named after its three main constituents quartz, feldspar and kaolinite. When a green porcelain body is heated, the kaolinite, brought in as clay, undergoes a dehydroxylation process at about 550°C (6) accompanied with some shrinkage (7) and amorphous metakaolinite is formed. At about 920°C feldspar begins to melt (8). This melting temperature is low in comparison

with the eutectic melting temperature of feldspar in the leucite-mullite-cristobalite phase diagram (6) because of various impurities (8). Starting at about 920°C, a spinel-type phase, amorphous silica and nanometer-sized primary mullite are formed almost simultaneously from the metakaolinite (9,10,11,12). With higher temperatures, the feldspar melt dissolves quartz and primary mullite. Secondary mullite is formed out of the melt from 1200°C onwards (6) and increases the rigidity of the body (2). The fired porcelain body contains partially dissolved quartz grains, mullite (both in primary and secondary form) and several glass phases of different composition.

2. Experimental Procedure

Two porcelain kilns have been analysed to examine the firing atmospheres. In a biscuit firing roller kiln, carbon dioxide has been measured by chemical methods. In a glost firing continuous furnace, the oxygen partial pressure has been measured by a ZrO_2 sensor (ZIROX GmbH, see (13)) travelling through the furnace with the setting. In both cases, partial pressures of the remaining gas components have been calculated.

To transfer the atmospheric conditions from gas fired production kilns to resistance heated laboratory furnaces, a gas mixing device and a gas analysis device have been constructed. The gas mixing device consists of four gas mass flow controllers (MFC) for air, hydrogen, nitrogen and carbon dioxide, a liquid mass flow controller for water and an evaporation device (CEM). The evaporation device brings together the flows of pre-mixed gas and liquid and evaporates the resulting flow by means of a heating device. The atmosphere at the sample position is controlled by a ZrO_2 oxygen partial pressure sensor (ZIROX GmbH).

Both the gas mixing and various gas analysis devices have been installed at the $MoSi_2$ laboratory furnace of a special thermooptical measuring system (TOM, (14)). The TOM allows for in-situ measurements of thermal diffusivity and sample shrinkage during sintering. Thermal diffusivity is measured by the laser-flash technique (15). Sample shrinkage is recorded simultaneously by an optical dilatometer.

Disk shaped samples were cut from isostatically pressed porcelain bodies, either in the green state or after biscuit firing. The measured chemical composition was 60.6 wt-% SiO_2, 32.1 wt-% Al_2O_3, 0.6 wt-% Fe_2O_3, 0.11 wt-% TiO_2, 0.27 wt-% CaO, 0.51 wt-% MgO, 1.62 wt-% Na_2O and 3.78 wt-% K_2O.

Green and biscuit fired samples were heated in the TOM to different biscuit and glost firing temperatures under different atmospheric conditions. Additional thermal analysis was carried out by DTA measurements (Setaram TAG 24) in dry air. Density of samples was measured by the Archimedes method. Formation of phases during firing was studied in a high-temperature X-ray diffractometer (see (4)) in dry air.

3. Results

The evolution of crystalline phases during heating of unfired porcelain, is shown in Fig. 1. Phase development was quantified by calculating the area under selected X-ray peaks (feldspar: $2\theta \approx 33.6°$,

kaolinite: 2θ≈12°, mullite: 2θ≈16.8°, quartz: 2θ≈21.5) recorded at different temperatures. The amount of kaolinite decreases from about 450°C up to 550°C where it becomes zero. The amount of feldspar drops to zero between 900°C and 1050°C. Mullite is formed above 950°C. The width of the mullite peaks is initially very broad. It decreases between 1150°C and 1250°C. The intensity of the quartz peaks decreases at temperatures above 1000°C.

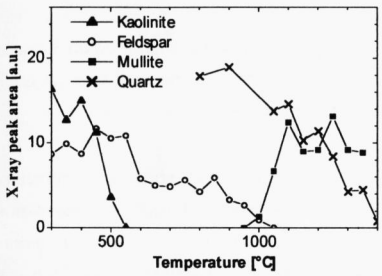

Fig.1: Phase formation during heating of porcelain measured by high-temperature X-ray diffractometry

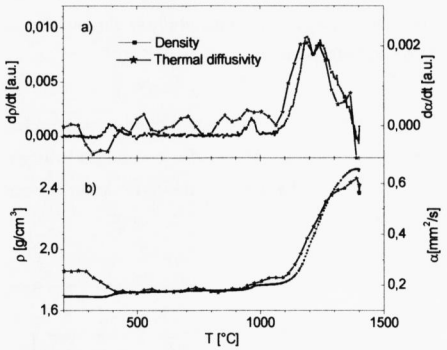

Fig.2: a) Densification rate dp/dt and differential thermal diffusivity d /dt and b) density p and thermal diffusivity during firing of a green porcelain sample (heating rate 2K/min)

Figure 2a) shows densification rates and the change of thermal diffusivities with time, both calculated from TOM measurements of sintering shrinkage and thermal diffusivity (Fig. 2b) of unfired porcelain in dry air. The curve for the densification rate shows three peaks at about 950°C, 1180°C and 1300°C, with a period of slower densification at 1240°C (see also (2,16)). The thermal diffusivity data closely follow the shrinkage data.

Whereas sample shrinkage stops between 980°C and 1080°C, the thermal diffusivity continuously increases from 900°C to 1050°C (Fig. 2b). At 1300°C the increase of the thermal diffusivity becomes smaller and is less than the increase of density (Fig. 2b).

Differential thermal analysis (DTA) shows that the peak temperatures during dehydroxylation of kaolinite (about 450°C) and the metakaolin transformation to primary mullite (about 1000°C) shift to higher values with increasing heating rates. Using the slopes of Arrhenius plots of heating rate vs. reciprocal peak maximum temperature for each of the two transformations, activation energies were calculated according to (7). They are 240 kJ/mol for the dehydroxylation and 1040 kJ/mol for the metakaolin transformation respectively.

Figure 3 shows a comparison of dry air with an industrial biscuit firing atmosphere containing 5 to 11 % water vapour during biscuit firing of porcelain. The thermal diffusivity of fired samples increases noticeably when the furnace atmosphere contains water vapour.

Fig. 3 also shows the effect of increasing biscuit firing temperatures on the thermal diffusivity of the resulting body. The effect of a firing atmosphere containing 17 vol-% water vapour on the densification behaviour of porcelain can be seen in Fig. 4 (the heating rate was 2 K/min). The three periods of enhanced sintering have been described before (Fig. 2a). The temperature of mullite formation, shown by the first period at about 950°C, is lowered by about 50 K under water vapour containing atmosphere. A similiar effect is also seen by DTA measurements of biscuit fired samples. Using dry air during biscuit firing, mullite formation takes place at more than 1050°C in the DTA measurement; using a biscuit firing atmosphere containing 17 vol-% water vapour, mullite formation begins at temperatures as low as 950°C.

The main shrinkage of the porcelain body also begins at lower temperatures when fired under water vapour containing atmosphere compared to dry air. The shrinkage rates of the third peak at about 1300°C are smaller when firing under water vapour containing atmosphere (Fig. 4).

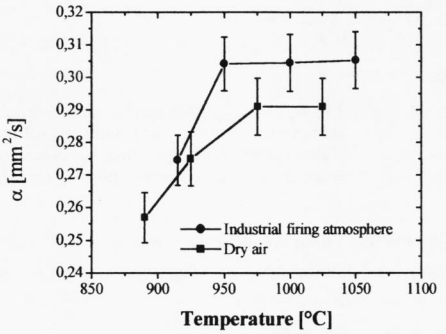

Fig.3: Thermal diffusivities α for different furnace atmospheres after biscuit firing of porcelain samples.

The sintering shrinkage has been measured for biscuit fired samples in the TOM under dry air for various constant heating rates up to temperatures of 1460°C. From this data the kinetic field (17) has been calculated (Fig. 5a). By connecting points of equal density on the sintering rate curves of different heating rates, the isodensity lines are constructed (Fig. 5a). From the slope of this lines the activation energy for densification has been calculated (Fig. 5b). The activation energy increases with progressive sintering.

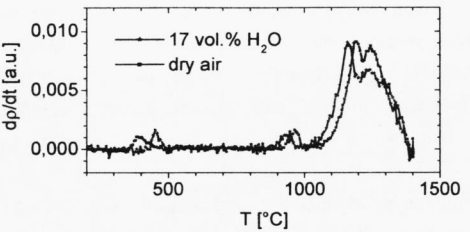

Fig.4: Densification rates of porcelain in dry air and water vapour containing atmosphere.

4. Discussion

The high temperature X-ray diffraction data (Fig. 1) are consistent with the literature results (cmp. section 1). The narrowing of the mullite peak at temperatures of about 1200°C is attributed to the transformation from primary to secondary mullite. The decrease in the feldspar intensity at 600°C is

attributed to the formation of a high-temperature modification (6). The shrinkage and thermal diffusivity data also fit to the general picture. From about 300°C to 400°C organic binder added to improve handling capabilities burns out, thereby lowering the thermal diffusivity as heat bridges between the particles are removed (Fig. 2b). Between 400°C and 550°C amorphous metakaolinite is formed from kaolinite (Fig. 1 and (6)). When feldspar begins to melt (at about 920°C (8)), the melt moves into particle contacts and noticeably increases the thermal diffusivity (Fig 2b). Penetration, fragmentation and rearrangement of the ceramic particles in this first liquid phase sintering stage (18) may lead to the small shrinkage observed between 920 °C and 980 °C (Fig. 2b). The shrinkage can be explained as well by the decomposition of metakaolinite to the spinel-type phase and primary mullite (12). To overcome sintering problems like cracks, it is important to ensure a homogeneous temperature distribution in this phase (1). In the temperature region between 980°C and 1050°C the formation of additional liquid phase from melting of feldspar does not effect the shrinkage, but further enhances the thermal diffusivity by strengthening the heat bridges between the solid particles.

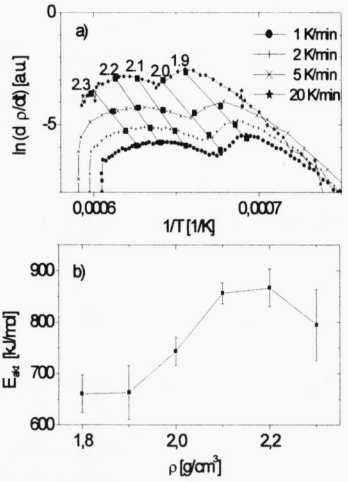

Fig.5 a) Kinetic field for the sintering of porcelain with heating rats of 1, 2, 5 and 20 K/min (the straight lines are isodensity lines denoted by the respective density in the range from 1.9 to 2.3 g/cm^3) and b) calculated activation energies of densification.

With higher temperatures quartz and clay minerals are dissolved into the melt, thereby increasing its viscosity. Secondary mullite which is formed from 1200°C onwards (6), further reinforces the microstructure. On the other hand, the viscosity of a feldspar melt of constant composition decreases with higher temperatures (2). It is attributed to this interplay of increasing and decreasing viscosity that the overall liquid phase sintering activity, shown by the densification rate, slows down for a short period at about 1240°C (Fig. 2a and Fig. 4). The increase in the activation energy for densification (Fig. 5b) is believed to reflect the same reinforcement. The activation energies are more than three times higher than the activation energy of about 200 kJ/mol (7) which has been calculated by assuming that viscous flow is the rate controlling mechanism of densification. Therefore, in our experiment other mechanisms like the speed of solution or diffusion in the liquid phase determine the shrinkage rate.

The presence of water vapour retards the dehydroxylation of kaolinite (Fig. 4) as is expected from thermodynamics. The two peaks at about 950°C and 1180°C are shifted to lower temperatures. This temperature shift is correlated with a decrease in the temperature of primary mullite formation

(determined by DTA, see section 3). This corresponds to the observation that the metakaolinite decomposition is favoured by the presence of water vapour (19). We assume that the viscosity of the liquid phase is lowered by the solution of water. This would shift the main shrinkage to lower temperatures in a water vapour containing atmosphere. The third peak in the shrinkage rate curve (Fig. 4) becomes smaller. This can be explained by the higher shrinkage which has already occurred at lower temperatures and demonstrates that the influence of water vapour is decreasing in this sintering stage.

5. Conclusions and outlook

The water vapour atmosphere in gas fired kilns enhances the sintering of porcelain bodies, resulting in denser microstructures at lower temperatures. This has to be considered if sintering experiments are to be transferred from resistance heated to gas fired furnaces. With the progresses in the field of kiln and burner design, even faster firing cycles will be possible in the near future. Using in-situ measuring methods for thermal diffusivity and sample shrinkage, the sintering kinetics of porcelain during glost firing has been examined and a kinetic field has been set up. With this knowledge it is possible to design rapid firing paths which avoid high shrinkage rates in regions of low strength and low thermal diffusivity (20). With sintering kinetic measurements one can also calculate the temperature distribution inside the porcelain body during firing. This distribution again effects sintering rates, heat conductivity and deformation.

6. Acknowledgements

The authors thank the Bayerische Forschungsstiftung for funding of this work (FORKERAM I-5). The help of S. Beyer, A. Klimera and N. Keidel with the measurements is gratefully acknowledged.

7. References

(1) D. Thiede: „Formstabilität von Porzellanmassen im Schnellbrand", Keramische Zeitschrift 50 [4] 1998, 249

(2) H. Mörtel, St. Krebs, K. Pham-Gia: „Examining Reaction Kinetics in the Fast Firing of Porcelain in Dependence from Different Raw Materials", cfi/Ber. DKG 77 (2000), No. 5, 26

(3) F. Raether: „Optimizing the Sintering Process via the Thermo-Optical Measuring Method", cfi ceramic forum int./Ber. DKG 75 No 10 (1998), 26

(4) L. Jacobsen, R. Hofmann, J. Zimmer, F. Raether, G. Müller: „In-situ Untersuchungen zur Sinterung von Aluminiumnitrid-Keramik", Beitrag zur Werkstoffwoche, Stuttgart, 1996

(5) G. Müller, F. Raether, L. Jacobsen: „Improvement of AlN ceramics by in situ measuring techniques", Proc. 9th Cimtec-World Ceramics Congress 1998, Ceramics: Getting into the 2000's - Part B, Techna Srl. (1999), 721

(6) W. M. Carty, U. Senapati: "Porcelain - Raw Materials, Processing, Phase Evolution and Mechanical Behaviour", J. Am. Cerm. Soc. 81 [1] 1998, 3

(7) S. M. Faieta-Boada, I. J. McColm: „Preliminary analysis of the thermal behaviour of an industrially used Ecuadorian clay", Applied Clay Science 8 (1993), 215-230

(8) S. T. Lundin: "Microstructure of Porcelain" (in "Microstructure of Ceramic Materials"), NBS Misc. Publ. 257 (1964), 93

(9) K. Okada, N. Otsuka, J. Ossaka: „Characterization of Spinel Phase Formed in the Kaolin-Mullite Thermal Sequence", J. Am. Ceram. Soc. Comm. 69 [10] 1986, C-251

(10) B. Sonuparlak, M. Sarikaya, I. Aksay: „Spinel Phase Formation During the 980°C Exothermic Reaction in the Kaolinite-to-Mullite Reaction Series", J. Am. Ceram. Soc. 70 [11] 1987, 837

(11) C. J. McConville, W. E. Lee, J. H. Sharp: „Microstructural evolution in fired kaolinite", Brit. Ceram. Trans. 97 (1998), 4, 162

(12) S. Lee, Y. Kim, H. Moon: „Phase Transformation Sequence from Kaolinite to Mullite Investigated by an Energy-Filtering Transmission Electron Microscope", J. Am. Ceram. Soc.82 [10] 1999,2841

(13) H.-H. Möbius, H. Sandow, K. Kämpfer, E. Prescher: „Grundlagen des Einsatzes von Festelektrolyt-Sonden in oxydierenden und reduzierenden Ofengasen beim Brennen von Keramik", Silikattechnik 41 (1990), 5, 169

(14) F. Raether, R. Hofmann, G: Müller, H. J. Sölter: „A novel thermo-optical measuring system for the in situ study of sintering processes", Journal of Thermal Analysis , Vol. 53 (1998), 717

(15) W. J. Parker et al.: "Flash Method of Determining Thermal Diffusivity, Heat Capacity and Thermal Conductivity", J. Appl. Phys. 32 (1961), 1679

(16) C. Y. Chen, G. S. Lan, W. H. Tuan: "Microstructural evolution of mullite during the sintering of kaolin powder compacts", Ceram. Int. 26 (2000), 715

(17) H. Palmour III, T. M. Hare, Sintering 85, Plenum Press N.Y. (1987), 17

(18) R. M. German: „Liquid phase sintering", Plenum Press, New York, 1985

(19) J. Temuuijn, K. Okada, K. J. D. MacKenzie, Ts. Jadambaa: "The Effect of Water Vapour Atmospheres on the Thermal Transformation of Kaolinite Investigated by XRD, FTIR and Solid State MAS NMR", J. Eur. Ceram. Soc. 19 (1998), 105

(20) F. Raether: „Microstructure development during sintering detected by novel in situ measuring techniques", Proceedings Sintering 1999, State College, PY, USA, 1999, to be published